

Magnetic Wave Interactions in a Periodically Corrugated YIG Film

S. R. SESHADRI, SENIOR MEMBER, IEEE

Abstract—The magnetic wave interactions in a YIG film having periodically corrugated surfaces are investigated for the case of magnetization parallel to the propagation direction. By a singular boundary perturbation procedure, the coupled-mode equations governing the nature of the interactions are deduced and analyzed to obtain the characteristics of the interactions. Representative numerical results are presented to reveal the characteristics of the resulting wave filter.

I. INTRODUCTION

MAGNETIZED epitaxial films of yttrium iron garnet (YIG) are used in the development of microwave signal processing devices [1], [2]. These devices are based on the characteristics of the magnetic waves guided by YIG films. An important feature is that the small propagation wavelengths of the magnetic waves result in microminiature structures. Extensive theoretical and experimental investigations of the characteristics of the magnetic waves supported by YIG films have been carried out for different directions of magnetization [3]–[8]. If the YIG films have spatially periodic properties, the guided waves propagating in opposite directions interact to produce a stopband in frequency resulting in a wave filter [9]. With application to a microwave filter in mind, Tsutsumi, Sakaguchi, and Kumagai [10] have investigated the behavior of the magnetic waves in a periodically corrugated YIG slab using the Floquet theory. In this paper, we give a perturbation theory of magnetic wave interactions in a YIG film having periodically corrugated surfaces for the case of magnetization parallel to the propagation direction. An important contribution is the systematic derivation of the coupled-mode equations governing the nature of the interactions. The analysis of the coupled-mode equations has yielded simple and yet asymptotically exact analytical expressions for the characteristics of the microwave filter formed by a periodically corrugated YIG film. Although the theory is developed for sinusoidal surface corrugations, in practice, an array of shallow grooves is etched on the surface of the YIG. For this case, by a Fourier analysis, the modulation index for each of the harmonic undulations of the surface can be deduced. The theory presented in this paper is then applicable for each of the harmonic surface perturbations.

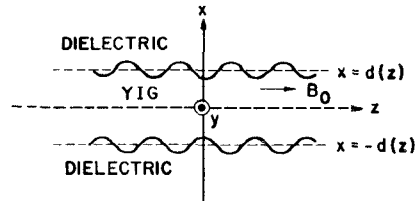


Fig. 1. Geometry of the periodically corrugated YIG film.

The sinusoidal corrugation corresponding to each of the harmonics gives rise to selective reflection and, hence, filtering action at a particular frequency.

II. FORMULATION OF THE PROBLEM

A thin film $[|x| < d(z)]$ of YIG ($\mu_0 \mu_r, \epsilon_0 \epsilon_n$) magnetized uniformly in the z direction is embedded in a dielectric medium (μ_0, ϵ_0) as shown in Fig. 1. The angular frequency corresponding to the saturation magnetization of the ferrite is denoted by ω_M and the corresponding wavenumber $k_M = \omega_M (\mu_0 \epsilon_0 \epsilon_r)^{1/2}$. We normalize the time by $1/\omega_M$, all the distances by $1/k_M$, the magnetic field by $(\mu_0)^{-1/2}$, and the magnetic flux density by $(\mu_0)^{1/2}$. Let $t, (x, y, z), \mathbf{H}$, and \mathbf{B} denote the normalized values of the time, the three Cartesian coordinates, the magnetic field, and the magnetic flux density, respectively. We shall consider only magnetic waves (H_x, H_z, B_x, B_z) progressing in the z direction, possessing no variation in the y direction, and having the time dependence $\exp(-i\omega t)$ where ω is the wave angular frequency. The relative permeability μ_r of the ferrite is obtained as

$$\mu_r = \mu_1 (\hat{x}\hat{x} + \hat{y}\hat{y}) + i\mu_2 (\hat{x}\hat{y} - \hat{y}\hat{x}) + \hat{z}\hat{z} \quad (1)$$

$$\mu_1 = 1 - \omega_c / (\omega^2 - \omega_c^2) \quad (2a)$$

$$\mu_2 = \omega / (\omega^2 - \omega_c^2) \quad (2b)$$

where ω_c is the gyromagnetic angular frequency.

The boundary surfaces $x = \pm d(z)$ of the YIG film have weak sinusoidal undulations about the planes $x = \pm d$ as given by

$$x = \pm d(z) = \pm d [1 + \delta\eta \cos Kz]. \quad (3)$$

The modulation index η , the phase, and the spatial periodicity $2\pi/K$ of the undulations are the same for both the surfaces $x = \pm d(z)$ with the result that the YIG film is symmetrical about the $x = 0$ plane. The modulation index η is small, and a formal expansion parameter δ is used to exhibit its smallness.

Manuscript received January 20, 1978; revised May 15, 1978.

The author is with the Department of Electrical and Computer Engineering, the University of Wisconsin-Madison, Madison, WI 53706.

In the magnetostatic approximation [3], [10], $\mathbf{H}(\mathbf{r})$ can be obtained in terms of a scalar magnetic potential $\psi(\mathbf{r})$ through the relation

$$\mathbf{H}(\mathbf{r}) = \nabla \psi(\mathbf{r}) \quad (4)$$

and $\mathbf{B}(\mathbf{r})$ inside the YIG and outside are given by

$$\mathbf{B}(\mathbf{r}) = \mu_r \cdot \mathbf{H}(\mathbf{r}), \quad \text{for } |x| < d(z) \quad (5a)$$

$$\mathbf{B}(\mathbf{r}) = \mathbf{H}(\mathbf{r}), \quad \text{for } |x| > d(z). \quad (5b)$$

A subscript f or v is added to ψ according to whether ψ pertains to the ferrite or the dielectric region. For $|x| < d(z)$, ψ_f satisfies the differential equation

$$\left(\mu_1 \frac{\partial^2}{\partial x^2} + \frac{\partial^2}{\partial z^2} \right) \psi_f(x, y) = 0. \quad (6)$$

The potentials and the fields have either odd or even symmetry about the $x=0$ plane. Since the geometry of the YIG film is also symmetrical about the $x=0$ plane, two independent modes are possible, one for which ψ is even in x , and the other for which it is odd in x . This symmetry enables us to omit from consideration the fields for $x < 0$. We investigate only the mode for which ψ is odd in x for the following two reasons. First, the lowest order mode for which ψ is odd in x is the dominant mode. Previously, for the mode for which ψ is odd in x , Tsutsumi, Sakaguchi, and Kumagai [10] have determined the wave characteristics by an approximation of the results of the Floquet theory. Since we wish to compare some of our results with those of Tsutsumi, Sakaguchi, and Kumagai [10], we also treat the same mode for which ψ is odd in x . However, it should be noted that the mode for which ψ is even in x can be treated in a similar manner.

A boundary layer expansion of ω as given by

$$\omega = \omega_0 + \delta \omega_1 \quad (7)$$

is introduced around ω_0 which will be chosen subsequently. Substituting (7) in (2a), expanding the resulting expression, and retaining only up to terms linear in δ , we get

$$\mu_1 = \mu_{10} + \delta \mu_{11} \quad (8)$$

where

$$\mu_{10} = 1 - \omega_c / (\omega_0^2 - \omega_c^2) \quad (9a)$$

$$\mu_{11} = 2\omega_c \omega_0 \omega_1 / (\omega_0^2 - \omega_c^2)^2. \quad (9b)$$

Using the method of multiple scales [11], we carry out a perturbation expansion of ψ in the form

$$\psi_t(x, z) = \psi_{t0}(x, z_0, z_1) + \delta \psi_{t1}(x, z_0, z_1), \quad t = v, f \quad (10)$$

where $z_0 = z$ is a short scale of the order of the wavelength in the YIG film and $z_1 = \delta z$ is a long scale in which the accumulated changes of the complex wave amplitude resulting from the spatially periodic thickness of the film become significant. Using the chain rule of differentiation, we have

$$\frac{\partial}{\partial z} = \frac{\partial}{\partial z_0} + \delta \frac{\partial}{\partial z_1}. \quad (11)$$

Substituting (8), (10), and (11) in (6) and equating the coefficients of equal powers of δ , we get the following differential equations:

0(1):

$$\left[\mu_{10} \frac{\partial^2}{\partial x^2} + \frac{\partial^2}{\partial z_0^2} \right] \psi_{f0} = 0 \quad (12)$$

0(δ):

$$\left[\mu_{10} \frac{\partial^2}{\partial x^2} + \frac{\partial^2}{\partial z_0^2} \right] \psi_{f1} = -\mu_{11} \frac{\partial^2}{\partial x^2} \psi_{f0} - 2 \frac{\partial^2}{\partial z_0 \partial z_1} \psi_{f0}. \quad (13)$$

In (6), (12), and (13), setting $\mu_1 = \mu_{10} = 1$ and $\mu_{11} = 0$, we obtain the corresponding equations for the dielectric region $|x| > d(z)$.

The required boundary conditions are

$$H_{\tan}(x, z) = H_z(x, z) + (dx/dz) H_x(x, z) \quad \text{is continuous for } x = d(z) \quad (14)$$

$$B_{\text{nor}}(x, z) = B_x(x, z) - (dx/dz) B_z(x, z) \quad \text{is continuous for } x = d(z). \quad (15)$$

From (3), (dx/dz) along $x = d(z)$ can be determined. With the help of (4), (5), (8), (10), and (11), the perturbation expansions of $H_{\tan}(x, z)$ and $B_{\text{nor}}(x, z)$ for $x = d(z)$ can be obtained. Since the boundaries of the YIG film are very nearly the planar surfaces $x = \pm d$, equivalent boundary conditions are derived and applied at the planar surfaces $x = \pm d$. For this purpose, further Taylor series expansions of the perturbation expansions of $H_{\tan}[d(z), z]$ and $B_{\text{nor}}[d(z), z]$ around $x = d$ are carried out, keeping only up to terms linear in δ . In these expansions, equating the coefficients of equal powers of δ , we obtain the following 0(1) and 0(δ) boundary conditions for $x = d$:

0(1):

$$\frac{\partial}{\partial z_0} \psi_{v0} = \frac{\partial}{\partial z_0} \psi_{f0} \quad (16)$$

$$\frac{\partial}{\partial x} \psi_{v0} = \mu_{10} \frac{\partial}{\partial x} \psi_{f0} \quad (17)$$

0(δ):

$$\begin{aligned} & \frac{\partial}{\partial z_0} \psi_{v1} + \frac{\partial}{\partial z_1} \psi_{v0} + d\eta \frac{\partial}{\partial z_0} \left\{ \cos Kz_0 \frac{\partial}{\partial x} \psi_{v0} \right\} \\ & \quad - Kd\eta \sin Kz_0 \frac{\partial}{\partial x} \psi_{v0} \\ & = \frac{\partial}{\partial z_0} \psi_{f1} + \frac{\partial}{\partial z_1} \psi_{f0} + d\eta \frac{\partial}{\partial z_0} \left\{ \cos Kz_0 \frac{\partial}{\partial x} \psi_{f0} \right\} \\ & \quad - Kd\eta \sin Kz_0 \frac{\partial}{\partial x} \psi_{f0} \end{aligned} \quad (18)$$

$$\begin{aligned} & \frac{\partial}{\partial x} \psi_{v1} + d\eta \cos Kz_0 \frac{\partial^2}{\partial x^2} \psi_{v0} + Kd\eta \sin Kz_0 \frac{\partial}{\partial z_0} \psi_{v0} \\ & = \mu_{11} \frac{\partial}{\partial x} \psi_{f0} + \mu_{10} \frac{\partial}{\partial x} \psi_{f1} + \mu_{10} d\eta \cos Kz_0 \frac{\partial^2}{\partial x^2} \psi_{f0} \\ & \quad + Kd\eta \sin Kz_0 \frac{\partial}{\partial z_0} \psi_{f0}. \end{aligned} \quad (19)$$

It should be noted that in (12), (13), and (16)–(19) the arguments of all the functions are x , z_0 , and z_1 .

III. ZEROTH-ORDER FIELDS

Using (12) and the requirement of boundedness of ψ_{t0} at $x = \infty$, we can express ψ_{t0} and ψ_{f0} as

$$\psi_{t0} = A_{0r} e^{-\beta_r(x-d)} e^{is\beta_r z_0} \quad (20)$$

$$\psi_{f0} = B_{0r} \frac{\sin k_r x}{\sin k_r d} e^{is\beta_r z_0} \quad (21)$$

where

$$k_r = \beta_r (-\mu_{10})^{-1/2}. \quad (22)$$

The wavenumber β_r is always taken to be positive and $s = 1$ or -1 according to whether the phase propagation is in the $+z$ or $-z$ direction. Let $[M]$ be a 2×2 matrix with the elements given by

$$M_{11} = -M_{12} = 1 \quad M_{21} = \beta_r \quad M_{22} = \mu_{10} k_r \cot k_r d \quad (23)$$

and $[F_{nj}]$ a 2×1 matrix with the elements A_{nj} and B_{nj} , which are functions of the slow space scale z_1 . The application of the boundary conditions (16) and (17) yields

$$[M][F_{0j}] = 0. \quad (24)$$

For a nontrivial $[F_{0j}]$, we obtain from (24) that

$$A_{0j} = B_{0j} \quad (25a)$$

$$\mu_{10} k_r \cot k_r d = -\beta_r \quad (25b)$$

where (25b) follows from the requirement that

$$\det [M] = 0. \quad (26)$$

The zeroth-order dispersion relation (25b) has solutions only for real values of k_r or negative values of μ_{10} . Then, (9a) shows that real β_r exists only in the frequency range

$$\omega_{01} = \omega_c < \omega_0 < [\omega_c(\omega_c + 1)]^{1/2} = \omega_{02}. \quad (27)$$

If β_r is a solution, $-\beta_r$ is also a solution of the zeroth-order dispersion relation. Using (22), we write (25b) conveniently as

$$\tan [\beta_r d(-\mu_{10})^{-1/2}] = (-\mu_{10})^{1/2}. \quad (28)$$

For each value of ω_0 lying within the range given by (27), there can be multiple solutions of β_r restricted to the regions

$$(j-1)\pi < \beta_r d(-\mu_{10})^{-1/2} < \left(j - \frac{1}{2}\right)\pi, \quad \text{where } j = 1, 2, 3, \dots \quad (29)$$

and the integer j gives the order of the waveguide mode. Let

$$v_g = \frac{d(\omega_0^2 - \omega_c^2)[\omega_c(\omega_c + 1) - \omega_0^2]}{\omega_0 [\beta_r d\omega_c + \omega_c(\omega_c + 1) - \omega_0^2]} \quad (30)$$

which is always positive for the frequency range given by (27). From (28), we can deduce that for $s=1$ (-1), the group velocity is given by $-v_g$ (v_g). Therefore, as is well

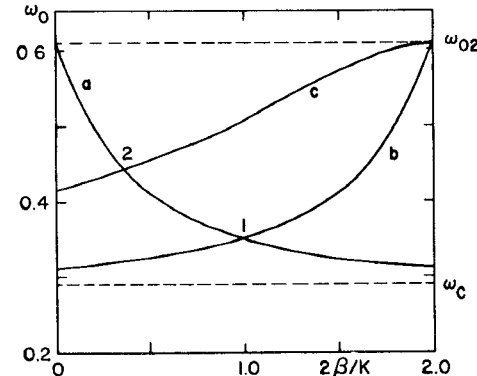


Fig. 2. Zeroth-order dispersion diagrams for $\omega_c = 0.290$ and $Kd = 2\pi$. *a*: fundamental Floquet mode having the wavenumber β_r with $r = 1$. *b*: first-order Floquet mode having the wavenumber $(-\beta_r + K)$ with $t = 1$. *c*: first-order Floquet mode having the wavenumber $(-\beta_r + K)$ with $t = 2$.

known [12], these guided magnetic waves are backward waves.

We shall investigate the contradirectional coupling and take the zeroth-order fields to be the superposition of the r th mode ($\beta_r = \beta_r$, $s = 1$) with its phase propagating in the $+z$ direction and the t th mode ($\beta_r = \beta_t$, $s = -1$) with its phase propagating in the $-z$ direction. From (20) and (21), the corresponding magnetic potentials are obtained as

$$\psi_{t0} = A_{0r}^+ e^{-\beta_r(x-d)} e^{i\beta_r z_0} + A_{0r}^- e^{-\beta_r(x-d)} e^{-i\beta_r z_0} \quad (31)$$

$$\psi_{f0} = B_{0r}^+ \frac{\sin k_r x}{\sin k_r d} e^{i\beta_r z_0} + B_{0r}^- \frac{\sin k_r x}{\sin k_r d} e^{-i\beta_r z_0} \quad (32)$$

where the superscripts on the wave amplitudes indicate the direction of phase propagation.

IV. COUPLED-MODE EQUATIONS

The boundary surfaces of the YIG film are periodically varying with the wavenumber K . Therefore, the Floquet theory [13] stipulates the dependence of the fields in the direction of periodic modulation and propagation to be of the form $\exp [i(\tilde{\beta} + nK)z]$ where $\tilde{\beta}$ is the fundamental wavenumber and the integer n running from $-\infty$ to ∞ gives the order of the Floquet mode. The zeroth-order fields are valid for the limiting case of vanishing modulation index for the boundary undulations. The wavenumbers β_r and $-\beta_r$ are the zeroth-order approximation to the fundamental Floquet modes. In Fig. 2, from (28), we have shown the zeroth-order dispersion curves for the fundamental Floquet mode with its phase propagating in the $+z$ direction and having the wavenumber β_r with $r = 1$ corresponding to the waveguide mode order 1, and the first-order Floquet mode with its phase propagating in the $-z$ direction and having the wavenumbers $(-\beta_t + K)$ with $t = 1$ and 2 corresponding to the waveguide mode orders 1 and 2. These zeroth-order dispersion curves intersect. The values of β_r , β_t , and ω_0 corresponding to each intersection point can be obtained from (28) and the relation

$$\beta_r = -\beta_t + K. \quad (33)$$

Near the intersection points the two phase-matched

zeroth-order Floquet modes interact. To understand the nature of these first-order contradirectional interactions we shall examine closely the neighborhood of the intersection points on an expanded scale. Therefore, in the boundary layer expansion of ω , ω_0 is chosen to coincide with the value of ω corresponding to the intersection point of the two zeroth-order dispersion curves.

From (12) and (13), the homogeneous first-order problem is seen to have a nontrivial solution as given by (31) and (32). Therefore, the inhomogeneous first-order problem has a solution if and only if certain solvability conditions are satisfied [14]. To determine the solvability conditions, we look for a particular solution of ψ_1 in the form

$$\psi_{1i} = g_{ir}(x)e^{i\beta_r z_0} + g_{tr}(x)e^{-i\beta_r z_0}, \quad i = v, f. \quad (34)$$

Substituting (31), (32), and (34) into (13) and using the orthogonality of the Floquet modes, for the Floquet mode $\exp(i\beta_r z_0)$, we get the differential equations satisfied by $g_{vr}(x)$ and $g_{fr}(x)$. Solving these differential equations subject to the requirement of boundedness of $g_{vr}(x)$ at $x = \infty$, we obtain that

$$\begin{aligned} g_{vr}(x) &= i \frac{\partial}{\partial z_1} A_{0r}^+ x e^{-\beta_r(x-d)} + A_{1r} e^{-\beta_r(x-d)} \quad (35) \\ g_{fr}(x) &= - \left[\frac{\mu_{11}}{\mu_{10}} k_r^2 B_{0r}^+ - \frac{2i\beta_r}{\mu_{10}} \frac{\partial}{\partial z_1} B_{0r}^+ \right] \\ &\quad \cdot \frac{x \cos k_r x}{2k_r \sin k_r d} + B_{1r} \frac{\sin k_r x}{\sin k_r d} \quad (36) \end{aligned}$$

where the coefficients A_{1r} and B_{1r} have to be determined from the $0(\delta)$ boundary conditions.

To obtain the boundary conditions for $g_{vr}(x)$ and $g_{fr}(x)$, (31), (32), and (34) are substituted into (18) and (19). With the help of (33), the functions of z_0 are written in terms of $\exp(i\beta_r z_0)$ and $\exp(-i\beta_r z_0)$. In view of the orthogonality, the boundary conditions should be satisfied for each of the Floquet modes separately. For the Floquet mode $\exp(i\beta_r z_0)$, the resulting boundary conditions, when simplified with the help of (22) and (25a) and (25b), are given by

$$g_{vr}(d) = g_{fr}(d) + \frac{1}{2} d \eta \frac{\beta_r}{\beta_r} (\beta_r + K) \left(1 - \frac{1}{\mu_{10}} \right) A_{0r}^- \quad (37)$$

$$\left\{ \frac{\partial}{\partial x} g_{vr}(x) \right\}_{x=d} = \mu_{10} \left\{ \frac{\partial}{\partial x} g_{fr}(x) \right\}_{x=d} - \frac{\mu_{11}}{\mu_{10}} \beta_r A_{0r}^+. \quad (38)$$

Let $[P_{\eta}]$ be a 2×1 matrix with the elements $p_{\eta 1}$ and $p_{\eta 2}$. When (35) and (36) are substituted into (37) and (38), we obtain that

$$[M] [F_{1r}] = [P_{1r}] \quad (39)$$

where

$$\begin{aligned} p_{1r1} &= -id \left(1 - \frac{1}{\mu_{10}} \right) \frac{\partial}{\partial z_1} A_{0r}^+ - \frac{\mu_{11} k_r^2 d}{\mu_{10} 2 \beta_r} A_{0r}^+ \\ &\quad + \frac{1}{2} d \eta \frac{\beta_r}{\beta_r} (\beta_r + K) \left(1 - \frac{1}{\mu_{10}} \right) A_{0r}^- \quad (40) \end{aligned}$$

$$p_{1r2} = \frac{\mu_{11} \beta_r}{2 \mu_{10}} (1 + \beta_r d) A_{0r}^+. \quad (41)$$

When (26) is used in (39), a relation is obtained between the elements of $[P_{1r}]$. This relation is one of the solvability conditions. With the help of (9a) and (9b) and (30), this solvability condition can be simplified and written as

$$\omega_1 A_{0r}^+ - iv_{gr} \frac{\partial}{\partial z_1} A_{0r}^+ = \eta C_{rt} A_{0r}^- \quad (42)$$

where

$$C_{rt} = -\beta_r (\beta_r + K) v_{gr} / 2 \beta_r. \quad (43)$$

Applying the boundary conditions for the Floquet mode $\exp(-i\beta_r z_0)$ and proceeding as before, we can deduce the second solvability condition in the form

$$\omega_1 A_{0r}^- + iv_{gr} \frac{\partial}{\partial z_1} A_{0r}^- = \eta C_{tr} A_{0r}^+. \quad (44)$$

The solvability conditions (42) and (44) are the coupled-mode equations governing the interaction of the zeroth-order Floquet modes $\exp(i\beta_r z_0)$ and $\exp(-i\beta_r z_0)$ resulting from the periodic undulations of the boundary surfaces of the YIG film.

V. FILTER CHARACTERISTICS

From (42) and (44), A_{0r}^+ and A_{0r}^- can be shown to satisfy the same differential equation. Substituting $A_{0r}^+ = A_{0r0}^+ \exp(i\beta_1 z_1)$ in that differential equation yields the following first-order dispersion relation:

$$\begin{aligned} \omega_1^2 + \omega_1 \beta_1 (v_{gr} - v_{gt}) - v_{gr} v_{gt} \beta_1^2 \\ - \frac{1}{4} \eta^2 (\beta_r + K) (\beta_r + K) v_{gr} v_{gt} = 0. \quad (45) \end{aligned}$$

Since for $\eta = 0$ it correctly reproduces the two group velocities, the first-order dispersion relation (45) is in the correct characteristic form.

The analysis of (45) shows that there is a stopband in frequency resulting from the interaction of the two modes. The guided wave is evanescent for $\omega_- < \omega < \omega_+$ where

$$\omega_{\pm} = \omega_0 \pm \frac{v_{gr} v_{gt} \{ (\beta_r + K) (\beta_r + K) \}^{1/2}}{(v_{gr} + v_{gt})} \eta. \quad (46)$$

At $\omega = (\omega_- + \omega_+)/2 = \omega_{\max} = \omega_0$, the maximum decay rate

$$(\beta_{1r})_{\max} = \{ (\beta_r + K) (\beta_r + K) \}^{1/2} \eta / 2 \quad (47)$$

occurs. In the evanescent region, the wavenumber is given by

$$\beta_{1r} = (\omega - \omega_0) (v_{gr} - v_{gt}) / 2 v_{gr} v_{gt} \quad (48)$$

and the decay rate can be expressed as

$$\begin{aligned} \beta_{1r} &= \frac{1}{2 v_{gr} v_{gt}} \left[(\beta_r + K) (\beta_r + K) v_{gr}^2 v_{gt}^2 \eta^2 \right. \\ &\quad \left. - (\omega - \omega_0)^2 (v_{gr} + v_{gt})^2 \right]^{1/2}. \quad (49) \end{aligned}$$

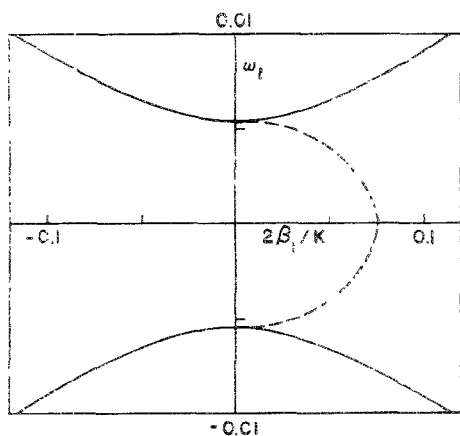


Fig. 3. Symmetric wave filter characteristics for the relative depth of the corrugations $\eta = 0.05$. Solid line—real wave number; dashed line—imaginary wave number. The coupling region corresponds to (1) in Fig. 2. $\omega_0 = 0.348$, $2\beta_r/K = 2\beta_i/K = 1.0$.

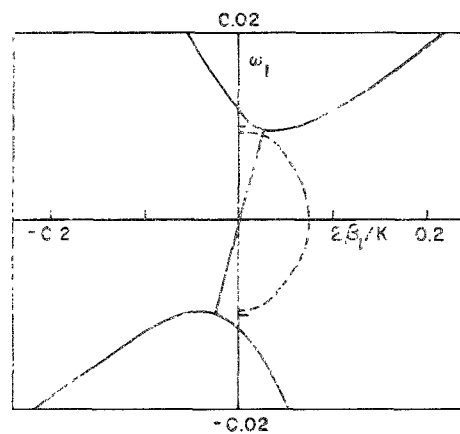


Fig. 4. Asymmetric wave filter characteristics for the relative depth of the corrugations $\eta = 0.05$. Solid line—real wave number; dashed line—imaginary wave number. The coupling region corresponds to (2) in Fig. 2. $\omega_0 = 0.442$, $2\beta_r/K = 0.365$, $2\beta_i/K = 1.635$.

The analytical expressions for the structure of the stopband show that the width of the stopband and the maximum decay rate increase linearly with the relative depth of the surface corrugations.

If the waveguide mode orders of the interacting modes are the same, $\beta_r = \beta_i = K/2$ and $v_{gr} = v_{gi}$, and the resulting interaction is known as a symmetric interaction. It is seen from (48) that in a symmetric interaction, the wavenumber remains a constant at its zeroth-order value throughout the evanescent region. Also, since $(\beta_{li})_{\max} = 3K\eta/4$, the maximum decay rate is independent of the thickness of the YIG film but is a linear function of the relative depth and the wavenumber of the periodic surface undulations. In an asymmetric interaction, $\beta_r \neq \beta_i$ and $v_{gr} \neq v_{gi}$ with the consequence that in the evanescent region, the wavenumber varies as a linear function of the frequency.

In Figs. 3 and 4, we have shown the characteristics of the interaction, respectively, for the coupling regions 1 and 2 pointed out in Fig. 2, and for the relative depth of the corrugations $\eta = 0.05$. The maximum decay rate al-

ways occurs at the center of the evanescent region. Using (33) and (47), we can show that the largest value of the maximum decay rate is obtained for a symmetric wave filter. No experimental results are available for comparison with our theoretical predictions. However, Tsutsumi, Sakaguchi, and Kumagai [10] have previously determined the characteristics of the symmetric wave filter by an approximation of the results of the Floquet theory. We chose the same physical parameters, namely, $Kd = 2\pi$, $\omega_c = 0.290$, and $\eta = 0.05$, as those used by the previous investigators [10] to facilitate comparison. The dispersion relation (24) of Tsutsumi, Sakaguchi, and Kumagai is accurate up to order η^2 . But in the approximations of the Bessel functions used in deducing the dispersion relation (24), the same required degree of accuracy has not been maintained with the result that the dispersion relation (24), strictly speaking, is not correct for the implied order of accuracy in terms of the relative depth of the surface corrugations. Consequently, their results for the symmetric wave filter agree only in general terms with those deduced here by a rigorous singular perturbation theory.

VI. CONCLUDING REMARKS

We have assumed the fields to have no variation in the y direction, that is in the direction of the width of the film, and have neglected the magnetic losses. All the important experimentally observed characteristics of magnetic waves on uncorrugated YIG films have been adequately explained by theories which neglect the field variations in the direction of the width of the film and magnetic losses [4], [6]. It is therefore to be expected that the major features of the characteristics of filters formed by corrugated YIG films can also be explained by a theory, such as the one presented in this paper, which assumes the fields to be uniform in the direction of the width of the film and which neglects the magnetic losses.

Magnetic waves on YIG films undergo attenuation due to surface roughness and induced strain between the film and the substrate. These losses are expected to be smaller for magnetic surface volume waves for which the energy is distributed throughout the thickness of the film as compared to magnetic surface waves for which the energy is concentrated on the surface of the film. As indicated by Adam and Collins [2] wide-band operation at X -band frequencies has necessitated the development of devices using magnetic surface volume waves. Such volume waves are obtained if the magnetization is parallel to the propagation direction. It is for this reason that we have chosen the magnetization to be parallel to the propagation direction.

A direct theoretical determination of the characteristics of a YIG film filter in terms of the physical parameters of the material and the geometry of the corrugations has remained an unsolved problem of great difficulty. For the first time in this paper we have presented a systematic and rigorous field theory for the characteristics of a magnetic film filter in terms of the material parameters, the geometry of the corrugations, and the frequency of operation.

We have also provided representative numerical results to emphasize the characteristics of the magnetic wave interactions. Although the present theory is rigorously valid only for a film of infinite length in the propagation direction, if the end effects are negligible, the coupled-mode equations can be used to deduce the insertion loss of a filter of finite length by imposing a phenomenological boundary condition on the wave amplitude.

ACKNOWLEDGMENT

The author is grateful to Dr. N. S. Chang for the extensive explanations of the research on magnetic wave interactions carried out at Osaka University during his recent visit to the University of Wisconsin.

REFERENCES

- [1] W. L. Bongianni, "X-band signal processing using magnetic waves," *Microwave J.*, vol. 17, no. 1, pp. 49-52, 1974.
- [2] J. D. Adam and J. H. Collins, "Microwave magnetostatic delay devices based on epitaxial yttrium iron garnet," *Proc. IEEE*, vol. 64, pp. 794-800, May 1976.
- [3] R. W. Damon and J. R. Eshbach, "Magnetostatic modes of ferromagnet slab," *J. Phys. Chem. Solids*, vol. 19, nos. 3-4, pp. 308-320, 1961.
- [4] L. K. Brundle and N. J. Freedman, "Magnetostatic surface waves on a YIG slab," *Electron. Lett.*, vol. 4, pp. 132-134, Apr. 1968.
- [5] S. R. Seshadri, "Surface magnetostatic modes of a ferrite slab," *Proc. IEEE*, vol. 58, pp. 506-507, Mar. 1970.
- [6] W. L. Bongianni, "Magnetostatic propagation in a dielectric layered structure," *J. Appl. Phys.*, vol. 43, no. 6, pp. 2541-2548, June 1972.
- [7] D. F. Vaslow, "Group delay time for the surface wave on a YIG film backed by a grounded dielectric slab," *Proc. IEEE*, vol. 61, pp. 142-143, Jan. 1973.
- [8] D. F. Vaslow, "Surface wave on a ferrite magnetized perpendicular to the interface," *IEEE Trans. Microwave Theory Tech.*, vol. MTT-22, pp. 743-745, July 1974.
- [9] C. Elachi, "Waves in active and passive periodic structures: A review," *Proc. IEEE*, vol. 64, pp. 1666-1698, Dec. 1976.
- [10] M. Tsutsumi, Y. Sakaguchi, and N. Kumagai, "Behavior of the magnetostatic wave in a periodically corrugated YIG slab," *IEEE Trans. Microwave Theory Tech.*, vol. MTT-25, pp. 224-228, Mar. 1977.
- [11] A. H. Nayfeh, *Perturbation Methods*. New York: Wiley Interscience, 1973, pp. 228-240.
- [12] B. Lax and K. J. Button, *Microwave Ferrites and Ferrimagnetics*. New York: McGraw-Hill, 1962, pp. 426-432.
- [13] L. Brillouin, *Wave Propagation in Periodic Structures*. New York: McGraw-Hill, 1946, pp. 172-175.
- [14] I. Stakgold, *Boundary Value Problems of Mathematical Physics*, vol. I. New York: Macmillan, 1967, pp. 82-86.

The Effects of Nonlinear Membrane Capacity on the Interaction of Microwave and Radio Frequencies with Biological Materials

GARY C. BERKOWITZ, STUDENT MEMBER, IEEE, AND FRANK S. BARNES, FELLOW, IEEE

Abstract—A model for the capacitance of biological membranes as a function of voltage is used to predict signal mixing and difference-frequency generation in membranes.

Production of low-frequency signals by the biomembrane from modulated RF is predicted, and implications for macroscopic modification of membrane function are discussed.

I. INTRODUCTION

RECENT realization of the significance of nonthermal interactions of radio and microwave frequency fields with biological materials generates a need for theo-

retical models to account for effects presently being observed [1]-[18]. Furthermore, the biological membrane is a likely locus for some of these effects [1], [4]-[6], [12]-[14], [16]-[18]. A model, based on the nonlinear conductance properties of the membrane, has been proposed to describe possible mixing phenomena and rectification [3].

In this paper, we examine voltage-variable membrane capacitance as another possible mechanism for generating difference frequencies. An approach taken is to treat the biological membrane as a "device" similar, in many respects, to a p-n junction diode as used in parametric amplifiers and harmonic generators. The characterization for the high-frequency response of the nonlinear capacitance is derived from low-frequency measurements on artificial membranes.

Manuscript received December 15, 1977; revised May 8, 1978.

The authors are with the Department of Electrical Engineering, University of Colorado, Boulder, CO 80309.